Two-photon double ionization of metastable $^{1,3}S$ $1s2s$ helium

A. S. Simonsen,[1,*] H. Bachau,[2] and M. Førre[1,†]

[1]*Department of Physics and Technology, University of Bergen, N-5007 Bergen, Norway*

[2]*Centre des Lasers Intenses et Applications, CNRS-CEA-Université de Bordeaux, F-33405 Talence Cedex, France*

(Received 21 March 2014; published 25 April 2014)

We investigate the process of two-photon double ionization (TPDI) of the metastable helium $^{1,3}S$ $1s2s$ states. The process has been simulated within a fully *ab initio* numerical framework, solving the time-dependent Schrödinger equation in full dimensionality for the two interacting electrons, in a B-spline-based methodology. The presence of doubly excited (autoionizing) states in the direct TPDI regime causes resonance-enhanced multiphoton ionization, and we demonstrate this effect by accessing the $^{1,3}P$ $2s2p$ doubly excited states. Fully converged theoretical calculations are presented, and a well-defined cross section is extracted for the direct TPDI process and compared in the context of its analogous process in the helium ground state. In addition, the resonance-enhanced two-photon double-ionization mechanism is explored, and we discuss how this process differs from both direct and sequential ionization processes.

DOI: 10.1103/PhysRevA.89.043427 PACS number(s): 32.80.Rm, 32.80.Fb, 42.50.Hz

I. INTRODUCTION

The problem of double photoionization of two-electron systems has undergone substantial investigations since the early work of Byron and Joachain [1]. The idea that one photon could eject two electrons from a bound system could only be attributed to the electron-electron interaction between a bound electron and an escaping photoelectron. The electron-electron interaction makes the multielectron wave function inseparable in the general case, and a detailed understanding of it, even in the simplest systems, is of great interest. Development of intense XUV sources through high-order-harmonic generation (HHG) [2,3] and free-electron lasers (FEL) [4,5] has provided experimentalists with the necessary tools to investigate double-ionization processes in few-electron systems. From a theoretician's point of view, the exponential increase in computing power during the last decades and the ability to perform large-scale multiprocessor numerical simulations have paved the way for exact theoretical treatment from first principles of such processes. When agreement between theoretical work and experiments was achieved for the problem of double photoionization of helium [6,7], much of the activity shifted to the problem of two-photon double ionization (TPDI). TPDI processes are not, in general, dependent on the electron-electron interaction if the ionizing laser has a photon energy which permits a sequential ejection of the electrons, i.e., single ionization of the target by one photon followed by ionization of the residual ion system by the second one. However, for a limited interval of photon energies, the total energy supplied to the system by two photons is only large enough to ionize both electrons if they are ejected simultaneously. This is called the direct or nonsequential regime. For example, in the case of TPDI of He($1s^2$), in the photon energy interval from 39.5 to 54.4 eV, TPDI is energetically allowed but cannot occur sequentially. This interval is of special interest as here the direct TPDI process can be studied separately from the sequential one. Being the simplest two-electron system, helium was the first target of considerable theoretical [8–25] and experimental [26–31] interest. Other two-electron systems have also been investigated, including TPDI of fixed-in-space H_2 [32–38].

It is clear that the processes of one- and two-photon double ionization have been studied to a great extent in several target systems, but mostly when the electrons originate from the system ground state. More recent activities include other initial states, for instance, the triplet and singlet He($1s2s$) states [39]. Also, double ionization due to single-photon impact has been investigated [40–42], along with TPDI in the sequential photon-energy regime [43] and TPDI of the ^3S $1s2s$ triplet state by two-color photons [44]. The two-photon breakup of He($1s2s$) is of particular interest since its dynamics differs significantly from the ordinary TPDI of He($1s^2$). Indeed, in the latter case TPDI is dominated, in zeroth-order perturbation theory for the electronic structure, by a two-photon transition of the type $1s^2 \to 1skp \to k'pkp$ [20,23]. The nature of direct TPDI of He($1s^2$) can be understood from the fact that the electron-electron repulsion is strongly present in the initial $1s^2$ state, and then the simultaneous ejection of the electrons will occur due to this additional repulsion energy. Furthermore, in the direct TPDI regime ($39.5 < \hbar\omega < 54.4$ eV), autoionizing states are located above the sequential threshold from the ground state of helium. As such, autoionizing states play a minor role in direct TPDI of He($1s^2$). Direct TPDI from He($1s2s$) (either singlet or triplet) involves, in zeroth-order perturbation theory, the channels $1s2s \to 1skp \to k'pkp$ and $1s2s \to 2skp \to k'pkp$. Using a perturbative treatment of the laser-atom interaction and a zero-order representation of the electronic states, it can be easily shown that these channels play a major role in the sequential TPDI regime [43], but they happen to cancel each other in the direct regime if the electron-electron interaction is neglected. On the other hand, autoionizing states like $2s2p$ can be directly populated through one-photon absorption. Therefore, and considering that the dipole coupling between the latter state and the initial $1s2s$ state is strong, the two-photon transitions of the types $1s2s \to 2s2p \to k'pkp$, $1s2s \to 2s2p \to k'sks$, and $1s2s \to 2s2p \to k'skd$ are expected to play a major role for photon energies below the sequential threshold. This will give rise to what is known as resonance-enhanced multiphoton

*aleksander.simonsen@ift.uib.no

†morten.forre@ift.uib.no

ionization (REMPI) when the central frequency of the driving field makes intermediate states resonant with the initial state. As we shall see, resonance-enhanced ionization cannot be treated as either a direct or a sequential process in the general case.

In this work, we present a theoretical investigation of the problem of two-photon double ionization of the metastable $^{1,3}S$ $1s2s$ states of helium. Employing a well-tested numerical scheme, we solve the time-dependent Schrödinger equation for the two-electron system in interaction with linearly polarized XUV laser pulses on the few-femtosecond time scale. The singlet and triplet states are studied systematically for different photon energies and laser pulse durations, and differences and similarities between these symmetries are noted. Both total (generalized) cross sections and energy- and angular-resolved differential cross sections are obtained in the direct (nonsequential) regime. Furthermore, the impact of the resonance-enhanced two-photon double-ionization (RE-TPDI) process, where doubly excited states play the role of the intermediate states, is studied in some detail. For instance, we show that whereas only one channel of total orbital angular momentum dominates in the direct regime, the resonance-enhanced process comprises two competing channels, indicating a different mechanism of ionization.

Atomic units where m_e, $\hbar$, e, and a_0 are scaled to unity are used throughout the paper unless stated otherwise.

II. THEORY AND METHODOLOGY

Our approach rests upon solving the time-dependent Schrödinger equation (TDSE) numerically to a high degree of accuracy for two-electron systems. The computational details of our scheme are described in [19], and it has been applied successfully to the study of various laser-induced processes in two-electron systems [19,20,24,36,45–47]. A short summary of the numerical details will be reiterated here for the convenience of the reader. The main idea revolves around representing the radial parts of the two-electron wave function in B splines, while handling the angular parts with the commonly used spherical expansion,

$$\Psi(r_1,r_2,\hat{\mathbf{r}}_1,\hat{\mathbf{r}}_2,t)=\sum_{i,j,k}c_{i,j,k}(t)\frac{B_i(r_1)}{r_1}\frac{B_j(r_2)}{r_2}\mathscr{Y}_k(\hat{\mathbf{r}}_1,\hat{\mathbf{r}}_2), \tag{1}$$

where $\mathscr{Y}_k(\hat{\mathbf{r}}_1,\hat{\mathbf{r}}_2)$ are the generalized spherical harmonics and k enumerates all combinations of l_1, l_2, L, and M satisfying the following condition:

$$|l_1-l_2|\leqslant L\leqslant l_1+l_2. \tag{2}$$

The full time-dependent Hamiltonian operator for the helium atom interacting with an electromagnetic field is expressed as the sum over one-electron contributions in addition to the electron-electron repulsion,

$$\widehat{H}=\sum_{i=1,2}\left(-\frac{\nabla^2_{\mathbf{r}_i}}{2}-\frac{2}{r_i}+\mathbf{A}(t)\cdot\mathbf{p}_i\right)+\frac{1}{|\mathbf{r}_1-\mathbf{r}_2|}. \tag{3}$$

Here $\mathbf{A}(t)$ represents the vector potential of the classical electromagnetic field within the dipole approximation. We model the laser pulse as a linearly polarized oscillating field with a sine-squared carrier envelope,

$$\mathbf{A}(t)=A_0\sin^2\left(\frac{t\pi}{T}\right)\cos(\omega t)\hat{\mathbf{u}}. \tag{4}$$

A_0 relates to the maximum electric field amplitude E_0 as $A_0=E_0/\omega$, with ω being the central angular frequency of the driving field. T corresponds to the full time duration of the laser pulse, whereas $\hat{\mathbf{u}}$ is the unit vector pointing in the direction of polarization. In the simulations, the pulse duration is varied for different photon energies and is given in numbers of optical cycles. At peak intensity, the laser pulse reaches $I_0=10^{13}$ W/cm^2, which produces a sufficiently strong signal in the double continuum while still being in the perturbative regime.

In order to locate the singly excited $^{1,3}S$ $1s2s$ states, we apply an implicit restarted Arnoldi method to the field-free Hamiltonian matrix where a shift parameter is adjusted in order to accelerate the convergence of the target energy eigenvalues. The time-dependent part of the problem is solved by propagating the TDSE with the Cayley-Hamilton propagation scheme,

$$\left(\mathbf{S}+\frac{i\Delta t}{2}\mathbf{H}(t+\Delta t)\right)\mathbf{c}(t+\Delta t)=\left(\mathbf{S}-\frac{i\Delta t}{2}\mathbf{H}(t)\right)\mathbf{c}(t), \tag{5}$$

where $\mathbf{S}$ is the overlap matrix and $\mathbf{H}$ is the Hamiltonian matrix in the basis described in Eq. (1). $\mathbf{c}(t)$ is the vector of expansion coefficients, and the process of time propagation is started with the initial vector $\mathbf{c}_0(t=0)$ corresponding to a field-free atomic eigenstate. Equation (5) is solved for the necessary amount of time steps in order to simulate the full extent of the laser-atom interaction and to obtain the final wave function Ψ_f.

The next challenge is to extract the physical observables, which relate to the process of TPDI, from the final wave function. First, the bound (initial state) component is removed. Then, the double-ionized wave packet is extracted by projecting the final wave function onto products of $Z=2$ Coulomb waves. The basic idea is to approximate the probability amplitude for a given angular channel and for a given set of continuum energies by the overlap between the final wave function and the product state spanned by two one-electron continuum states,

$$P_{l_1,l_2,L,M}(E_1,E_2)=\left\langle\psi^{Z=2}_{E_1,l_1}(\mathbf{r}_1)\middle|\left\langle\psi^{Z=2}_{E_2,l_2}(\mathbf{r}_2)\middle|\Psi_f^{l_1,l_2,L,M}(\mathbf{r}_1,\mathbf{r}_2,t=\tau)\right\rangle\right., \tag{6}$$

where τ is some time after the conclusion of the laser pulse. Indeed, the electron-electron correlation is not built into such product states, but in the asymptotic regime where the electrons are spatially well separated, the electron-electron interaction plays a minor role. The accuracy of this method has been investigated (see, for instance, [16,24]), and it is found that the associated error is small and can be controlled by a technique known as postpropagation. The idea is simply to expose the final wave function to field-free time propagation in order to let the ionized electrons drift apart and hence reduce the importance of the electron-electron repulsion in

the continuum components. The fully angular- and energy-resolved probability amplitude is then obtained as [11,16,48],

$$P(E_1,E_2,\Omega_1,\Omega_2) = \sum_{l_1,l_2,L,M} e^{-\frac{i\pi}{2}(l_1+l_2)+i(\sigma_{l_1}+\sigma_{l_2})} \times \mathscr{Y}^{L,M}_{l_1,l_2}(\Omega_1,\Omega_2) P_{l_1,l_2,L,M}(E_1,E_2), \quad (7)$$

where $\sigma_l = \Gamma(1+l-iZ/\sqrt{2E})$ is the Coulomb phase shift. The relationship between the probability amplitude and the (differential) generalized cross section for a two-photon process is given by

$$\sigma = \left(\frac{\omega\hbar}{I_0}\right)^2 \frac{|P|^2}{T_{\rm Eff}}, \quad (8)$$

where I_0 is the intensity of the field at maximum amplitude and the quantity $T_{\rm Eff}$ is the effective pulse duration. For a pulse with a sine-squared carrier envelope it is given as $T_{\rm Eff} = 35T/128$ [49]. Any future use of the term "cross section" refers to this generalized one.

III. RESULTS AND DISCUSSION

The initial $^{1,3}S$ $1s2s$ helium states were obtained in a radial box extending up to 280 a.u. with 290 B-spline functions in each radial coordinate. The two-electron wave function is resolved in all single-electron orbital angular momentum combinations (l_1,l_2) up to $l_1 = l_2 = l_{\rm max} = 12$. We obtain the binding energies $E = 58.39$ eV and $E = 59.19$ eV for the singlet and triplet $1s2s$ states, respectively. The eigenenergies of the $1s2s$ and $2s2p$ states as well as the autoionization properties of the latter are summarized in Table I. In terms of convergence, we have systematically adjusted the discretization parameters in order to ensure that the results are not sensitive to the basis. It turns out that $l_{\rm max} = 6$ is sufficient in order to obtain converged total cross sections. As expected, the angular-resolved results are much more sensitive to the number of angular channels included. In fact, only between $l_{\rm max} = 10$ and $l_{\rm max} = 12$ do the angular distributions seem to be quantitatively identical, while lower $l_{\rm max}$ is able to capture the qualitative shape. The B-spline density has been varied as well, and the results are found to be converged. The box size is adjusted in order to fit the continuum wave packets produced during the propagation of the TDSE, and longer laser-atom interactions necessitate larger radial boxes. Also, as explained in Sec. II, the process of extracting the double-continuum component is associated with an error which is controlled by the postpropagation technique. As found in similar studies [16,24], the error is relatively small (of the order of a few percent) and diminishes rapidly only with a few cycles of postpropagation.

TABLE I. Energies and widths of the states accessed in the two-photon double-ionization process. The energies and widths of the autoionizing states are found in [50].

Quantity	Singlet	Triplet
$1s2s$ energy	−58.39 eV	−59.19 eV
$2s2p$ energy	−18.86 eV	−20.69 eV
$1s2s$-$2s2p$ energy gap	39.46 eV	38.50 eV
$2s2p$ lifetime	17.8 fs	82.3 fs
$2s2p$ width	0.037 eV	0.008 eV

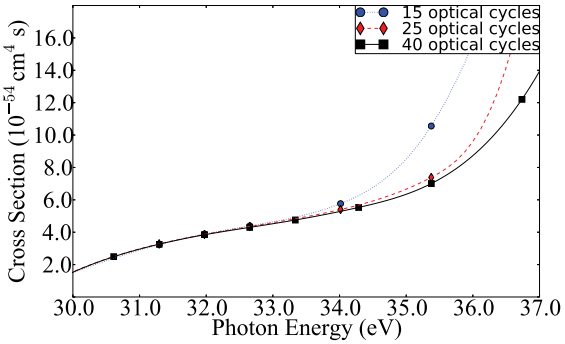

FIG. 1. (Color online) Total (generalized) cross section for the process of direct two-photon double ionization of the metastable ^1S $1s2s$ state, as obtained for laser pulses of 15- (dotted blue line with circles), 25- (dashed red line with diamonds) and 40-cycle (solid black line with squares) duration and peak intensity of 10^{13} W/cm^2.

The lower direct TPDI threshold is given as half the initial binding energy because the two photons together must supply the necessary energy to doubly ionize the target. Strictly speaking, direct TPDI is energetically possible for all photon energies above this limit, but an upper threshold for direct TPDI is conveniently defined as the lower threshold for sequential TDPI. This is natural as the sequential process tends to dominate the direct one whenever both are open. The upper direct or lower sequential threshold is defined by requiring that the first photon has enough energy to produce an ion state from the initial state and that the second photon is sufficiently energetic to ionize the same respective ion state. In the singlet (triplet) case, direct and sequential TPDI open at photon energies of 29.2 (29.6) and 44.8 (45.6) eV, respectively. The process of two-photon double ionization is usually classified according to these two types of ionization dynamics, i.e., sequential and direct, but in the He ($1s2s$) case, one must also consider a third possibility, namely, RE-TPDI, which does not behave exactly like the direct or the sequential process. At first sight, the RE-TPDI process may look very similar to the sequential one, merely due to the consecutive order of the photon absorption. However, it should be pointed out that in the RE-TPDI case, both electrons are still quasibound in the intermediate autoionizing state, and as such, the electrons are double ionized simultaneously, similar to the case of the direct process.

A. Total cross section

Figure 1 shows the total (generalized) TPDI cross section as a function of photon energy for the singlet case and for three different pulse durations. Notice how the cross section seems well defined for photon energies below 34 eV as the results obtained with different pulse durations align with each other. However, above 34 eV the cross section is obtained as a pulse-dependent quantity, and as we shall see, this is caused by a nearby doubly excited state, namely, ^1P $2s2p$. In the continuation, we will discuss the two-photon

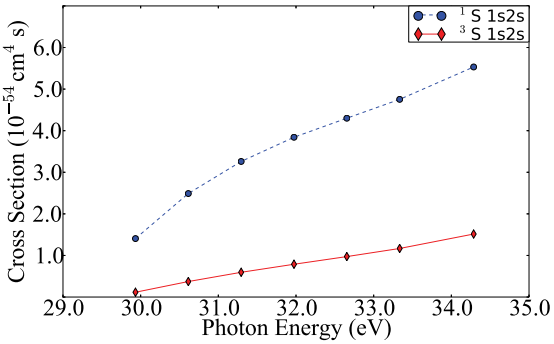

FIG. 2. (Color online) Total (generalized) cross section for the process of direct two-photon double ionization of the ^1S $1s2s$ singlet (dashed blue line with circles) and ^3S $1s2s$ triplet (solid red line with diamonds) states, respectively, as obtained for a 40-cycle laser pulse of peak intensity $I_0 = 10^{13}$ W/cm^2.

double-ionization process in both regions, starting with the region below 34 eV where the cross section is well defined for the laser pulses considered here.

1. Direct TPDI

Figure 2 depicts the total TPDI cross section for both the singlet (dashed blue line with circles) and triplet (solid red line with diamonds) $1s2s$ states, as obtained for a laser pulse of 40-cycle duration. Their numerical values are also given in Table II. The cross sections were extracted 10 optical cycles after the conclusion of the pulse in order to ensure that the double-ionized wave-packets comprise well-separated electrons. The most obvious observation is that the TPDI cross section obtained in the singlet symmetry is categorically larger compared to that of the triplet. In addition, the cross sections in both symmetries are significantly smaller than in the case of TPDI of the helium ground state [16,19]. The difference in magnitude can be attributed to the electron-electron interaction, which is a prerequisite for the double ionization to occur, and the fact that the electron-electron correlation is relatively more important in the helium ground state. The difference in magnitude between the singlet and triplet yields is explained by the symmetry properties of the states, which again give rise to a similar effect: In the triplet case, the wave function vanishes at $\mathbf{r}_1 = \mathbf{r}_2$ due to its spatial antisymmetry, and as such the importance of the electron-

TABLE II. The total (generalized) cross section vs photon energy for the process of direct two-photon double ionization of the $^{1,3}S$ $1s2s$ states. The cross section is given in units of 10^{-54} cm^4 s.

Photon energy (eV)	Singlet cross section (10^{-54} cm^4 s)	Triplet cross section (10^{-54} cm^4 s)
29.9	1.41	0.12
30.6	2.49	0.37
31.3	3.26	0.60
32.0	3.84	0.79
32.7	4.30	0.97
33.3	4.75	1.17
34.3	5.53	1.52

electron repulsion is suppressed, with the consequence that the TPDI yield declines.

2. Resonance-enhanced TPDI

Turning to photon energies above 34 eV, the ionization process is influenced by the intermediate $2s2p$ doubly excited state. As already mentioned, the presence of doubly excited states in the middle of the direct regime for TPDI necessitates a different treatment for photon energies close enough that such states are populated. The interpretation of "close" in this context is dependent on the spectral distribution of the laser pulse, i.e., the photon energy, and also the pulse duration and shape. One of the most profound differences between the direct regime for TPDI and the resonance-enhanced counterpart is how the probability of ionization scales with the duration of the laser pulse. For the direct case, no intermediate physical atomic or ionic states are accessed by the first photon, which is in direct contrast to the RE-TPDI case where intermediate doubly excited states are significantly populated during the interaction. The population in bound intermediate atomic states is, within the lowest order of perturbation theory, expected to be proportional to T^2 once they are accessed by the field. For autoionizing states, the picture is more complicated, and the relationship between the population and the duration of some photon-driven excitation is dependent on the time scale of the pulse with respect to the time scale for autoionization, i.e., the decay rate of the relevant states. As such, the probability for double ionization by two photons will, in general, depend on the population in the intermediate state and scale by some power of the pulse duration larger than 1. The probability for TPDI of He(^1S $1s2s$) versus photon energy is shown in Fig. 3 for three different pulse durations, 15 (dashed blue line), 25 (dotted red line), and 40 (solid black line) optical cycles of illumination. The RE-TPDI process is clearly expressed around $\hbar\omega = 39.5$ eV as a resonance peak, and here the probability scales with the pulse duration beyond the first order (a similar resonance peak is also present in the triplet case [44]). As already mentioned, the extent of the

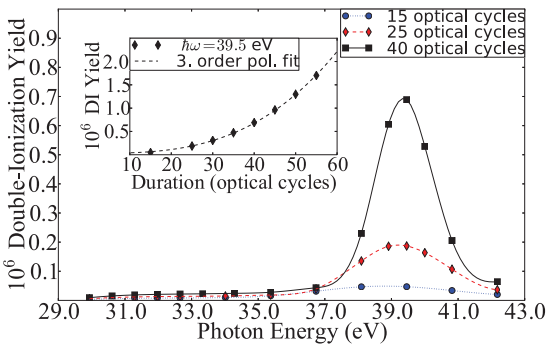

FIG. 3. (Color online) Total TPDI yield vs photon energy for the ^1S $1s2s$ state, as obtained for laser pulse durations of 15 (dotted blue line), 25 (dashed red line), and 40 (solid black line) optical cycles. The inset shows the total TPDI yield vs pulse duration (given in optical cycles) at the resonant photon energy $\hbar\omega = 39.5$ eV. The dashed black curve shows the best least-squares fit of the form $aT^3 + b$, illustrating the cubic relationship between the total ionization probability and the laser pulse duration.

resonant regime is pulse dependent; that is, the peak obtained with the 40-cycle pulse is somewhat sharper compared to the 25- and 15-cycle peaks. The inset in Fig. 3 displays the total TPDI probability as a function of pulse duration for the photon energy $\hbar\omega = 39.5$ eV, which is the resonant photon energy for the transition $^1S\ 1s2s \rightarrow {}^1P\ 2s2p$. Polynomial regression reveals that the data points are best approximated by a polynomial fit of the form $aT^3 + b$, indicating a T^3 dependence. The cubic dependence on pulse duration is a characteristic of the underlying ionization mechanism. The mean lifetimes of the $^{1,3}P\ 2s2p$ states are of the order of several tens of femtoseconds (see Table I), which is long compared to the few-femtosecond duration of the laser pulse. Therefore, the resonance states appear long-lived and sharply defined with respect to the duration and spectral width of the pulse, and as such they behave as true bound states in the few-femtosecond regime. For very long pulses, i.e., when the spectral width of the pulse becomes comparable to that of the intermediate states, the two-photon double-ionization probability is again expected to scale linearly, and not cubicly, with the pulse duration, and the notion of a generalized cross section again becomes a meaningful quantity.

B. Differential cross sections

More information about the underlying two-photon breakup mechanisms may be revealed by studying the partial-wave decomposition as well as differential observables. One interesting feature can be observed by considering the relative importance of the two competing channels $L = 0$ and $L = 2$ as a function of photon energy. It was shown in Refs. [11,51] that the two total angular momentum components contribute with similar weight in the process of TPDI of the helium ground state, even for photon energies close to the lower TPDI threshold. Also, in the case of the helium ground state, the two electrons absorbing one photon each is suggested as the primary mechanism of ionization [20,52], leading naturally to a dominant angular pair pp and $L = 0,2$. Then other angular pairs $(ss,sd,\ldots)$ are populated due to the electron-electron interaction, and the mixture of these configurations leads to asymmetric angular distributions in the double continuum [11,53].

The total angular momentum decompositions for the double-continuum wave packet, with $^{1,3}S\ 1s2s$ targets, are shown in Fig. 4 as a function of photon energy. The competing channels $L = 0$ (dashed lines) and $L = 2$ (solid lines) are shown for the singlet (blue lines with circles) and triplet (red lines with diamonds) symmetries in the photon energy interval from 29 to 44 eV. It is clear that the partial waves contribute to the double-ionization yield to different degrees for the various photon energies. Whereas mainly the $L = 2$ component is important for lower photon energies, both $L = 0$ and $L = 2$ are important in the region of the $2s2p$ resonance. A physical interpretation for this is found in the different available ionization routes between the $^{1,3}S\ 1s2s$ and the double continuum with and without the intermediate resonance states. Below resonance, the $1s$ electron is favored to absorb two photons since it is more strongly bound than the $2s$ electron, and hence, part of the excess energy is transferred to the $2s$ electron via a collisional process which ionizes it. It

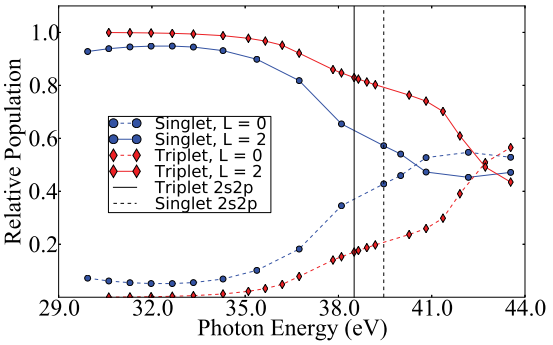

FIG. 4. (Color online) Partial-wave decomposition of the double continuum with respect to the total angular momentum $L = 0$ and 2 for the process of two-photon double ionization of the metastable $^{1,3}S\ 1s2s$ states. The population in each channel is normalized with respect to the total TPDI yield (see Fig. 3). The singlet and triplet symmetries are indicated by blue lines with circles and red lines with diamonds, respectively. The positions of the $2s2p$ resonances in both the singlet and triplet symmetries are indicated by vertical lines.

is worth noticing that in the case of two-photon sequential double ionization of He$(1s2s)$, the channel where the $1s$ electron is first ionized also dominates over the one where the $2s$ electron absorbs the first photon when both channels are energetically open for sequential TPDI [43]. Furthermore, the large $L = 2$ component in the case of direct TPDI can be understood from the simpler process of two-photon (single) ionization of the $He^+(1s)$ state, where mainly the $l = 2$ component in the continuum is populated due to the strong dipole coupling between the $2p$ (virtual intermediate state) and the $l = 2$ (continuum) states. In contrast, when the $2s2p$ state is resonant, the $1s$ electron absorbs the first photon and accesses the $2s2p$ state. Then, the second photon is absorbed from the $2s2p$ state by either the $2s$ or the $2p$ electron, leading to a more even distribution in the $L = 0$ and $L = 2$ channels.

Even if the total energy and momentum of the system are conserved in a two-photon double-ionization process, the individual electrons share the excess energy and momentum in different ways. As such, we will now focus on differential observables which are presented in units of cross section for both the direct and resonance-enhanced processes. Strictly speaking, in the latter case the cross section is not a well-defined quantity due to the T^3 scaling of the corresponding TPDI yield, but we still find it a useful quantity here in order to compare shapes and relative TPDI yields for the different processes on an equal footing.

1. Single-differential cross section

Figure 5 shows the single-differential cross section (SDCS) for four different photon energies for both the singlet (left panel) and triplet (right panel) symmetries. The SDCS is resolved in the quantity $E_1/(E_1 + E_2)$, i.e., the relative energy sharing between the electrons, with E_1 and E_2 being the energies of electrons 1 and 2. The general shape of the SDCS is a U-shaped curve, indicating that equal energy sharing between the double-ionized electrons is the least probable outcome of the TPDI process. As it turns out, the U-shape behavior is

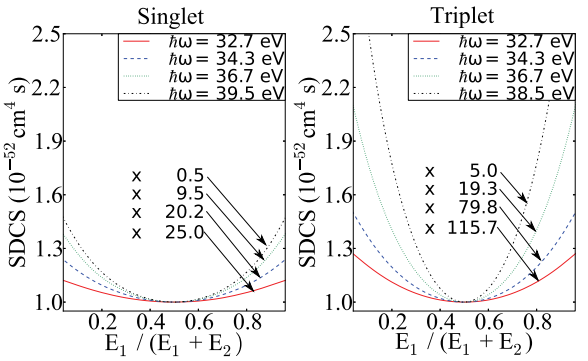

FIG. 5. (Color online) Single-differential cross section (SDCS) vs $E_1/(E_1+E_2)$, i.e., relative energy sharing between the outgoing electrons, for the process of two-photon double ionization of (left) ^1S $1s2s$ and (right) ^3S $1s2s$. The SDCS is obtained for four different photon energies and has been scaled with the indicated factors for comparison.

typical for direct TPDI processes in general and has already been observed in other two-electron systems [11,36,47].

As seen in Fig. 5, the general trend is that for higher photon energies the probability for asymmetric energy sharing becomes more and more pronounced, which is revealed as sharper U shapes. Comparing the left and right panels in Fig. 5, i.e., the singlet and triplet scenarios, respectively, equal energy sharing turns out to be much more likely in the singlet case, indicating a higher degree of energy transfer between the electrons. This is partially attributed to the nodal behavior of the triplet wave function at $\mathbf{r}_1 = \mathbf{r}_2$, which suppresses the ability for energy transfer between the electrons as they are less likely to be close to each other. There is little evidence of the resonance-enhanced process in the shapes of the SDCSs. As such, the presence of the intermediate doubly excited states does not seem to significantly alter the degree of electron-electron energy transfer.

2. *Triple-differential cross section*

Turning to fully energy- and angular-resolved observables, Fig. 6 depicts the conditional triple-differential cross section (TDCS), where the energy of electron 2 is integrated out, as obtained for the singlet (left panels) and triplet (right panels) symmetries. The photon energy $\hbar\omega = 32.7$ eV, which falls into the direct regime. In the spectra, the azimuthal angles of both electrons are fixed at $\phi = 0$, and electron 1 is assumed to escape with the polar angles $\theta_1 = 0°$, $30°$, $60°$, and $90°$ (from top to bottom in the figure) with respect to the direction of polarization. The energy of electron 1 is fixed at one-half, one-fourth, one-sixth, and one-eighth of the total excess kinetic energy. Comparing the two symmetries, clear differences in their respective angular distributions are expressed. Focusing on equal energy sharing first (dashed red curves), direct back-to-back emission is an important contribution in the singlet symmetry, but it is completely absent in the triplet case (see rule C in [54]). A similar observation was pointed out by Armstrong and Colgan for the case of TPDI in lithium [55]. The phenomenon is also manifested as a selection rule for the ^3D continuum, which is the only accessible continuum at equal energy sharing due to the Pauli exclusion principle (see rule E

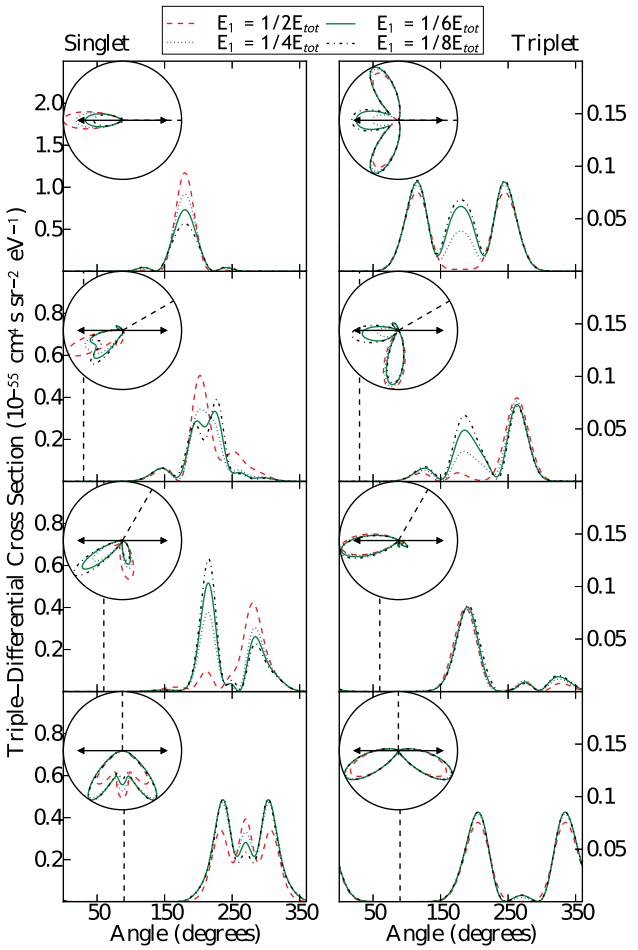

FIG. 6. (Color online) Triple-differential cross section (TDCS) for the process of direct two-photon double ionization of the helium (left) ^1S $1s2s$ and (right) ^3S $1s2s$ states, obtained with $\hbar\omega = 32.7$ eV, a 40-cycle laser pulse, and $l_{\max} = 12$. One of the electrons (electron 1) is assumed to be emitted at $0°$, $30°$, $60°$, and $90°$ (from top to bottom) with respect to the laser polarization axis. The energy of electron 1 is fixed at one-half, one-fourth, one-sixth, and one-eighth of the total excess kinetic energy, and the energy of electron 2 is integrated out. The dashed vertical lines show the prefixed escape direction of electron 1, whereas the black arrows in the polar plot indicate the axis of polarization.

in [54]). When electron 1 escapes with a smaller fraction of the excess energy, the angular spectra in the singlet vary to some degree, mostly in the back-to-back directions, but the overall shape is similar. In the triplet, the selection rules imposed for equal energy sharing are no longer valid, and back-to-back emission emerges along the axis of polarization. Moreover, the TDSC seems almost identical, hence independent of the energy sharing, when electron 1 is ejected with a dominating perpendicular component with respect to the laser polarization direction ($\theta_1 = 60°$ and $\theta_1 = 90°$). As such, ejection of high- and low-energy pairs of electrons into the triplet continuum is biased towards scattering directions where both electrons escape with an angle close to the axis of polarization.

Figures 7 and 8 depict the TDCS at photon energies of 39.5 and 38.5 eV for the singlet (Fig. 7) and triplet (Fig. 8) symmetries, respectively. The photon energies are chosen to

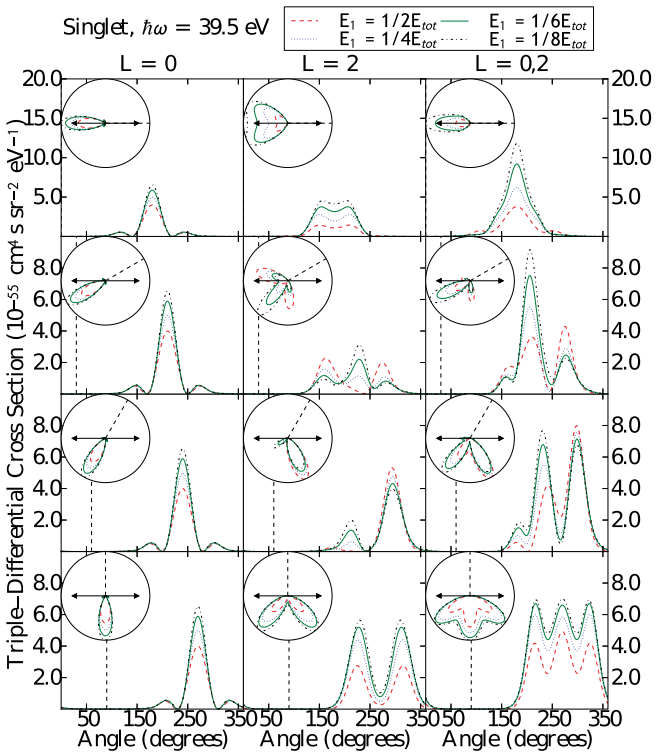

FIG. 7. (Color online) Same as Fig. 6, but for the singlet case with photon energy of 39.5 eV, which makes the $^1S\ 1s2s \rightarrow {}^1P\ 2s2p$ transition resonant. (left) The partial TDCS from the $L = 0$ channel. (middle) The partial TDCS from the $L = 2$ channel. (right) The total TDCS from both the $L = 0$ and 2 channels.

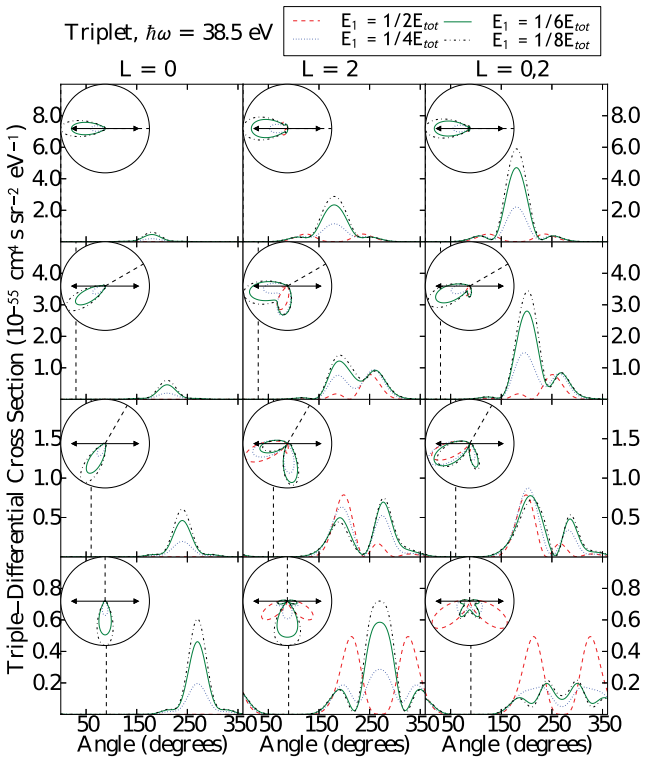

FIG. 8. (Color online) Same as Fig. 7, except for the $^3S\ 1s2s$ target state. Here, the photon energy is 38.5 eV, which resonantly drives the transition $^3S\ 1s2s \rightarrow {}^3P\ 2s2p$.

be equal to the excitation energies of the $^{1,3}P\ 2s2p$ doubly excited states, making the processes examples of RE-TPDI. The left panels show the relative contribution of the $^{1,3}S^e$ ($L = 0$) double-continuum channel, the middle panels show the contribution from $^{1,3}D^e$ ($L = 2$), and the right panels show the coherent superposition of the two, i.e., the total TDCS. For the case of equal energy sharing (dashed red curves), the overall shape of the angular spectra (rightmost panels) is quite similar to those obtained in the purely direct TPDI process (see Fig. 6). However, by allowing electron 1 to escape with a fraction of the excess energy not equal to one-half, the situation is quite different: The general effect on the TDCS, caused by the intermediate $^{1,3}P\ 2s2p$ doubly excited states, now seems to be an overall increased tendency for back-to-back scattering in both symmetries. The lobes which pertain to direct back-to-back scattering tend to increase with an increasing degree of unequal energy sharing, independent of the escape direction of electron 1. This is associated with a larger relative population in the $^{1,3}S$ continuum compared to the one in the direct TPDI process and can be explained by the fact that in the resonant case the second photon is absorbed by the $2s$ or $2p$ electron in the $^{1,3}P\ 2s2p$ state with similar probability. As such, the $L = 0$ component plays a more significant role for the resonant photon energy (see Fig. 4), and its contribution comprises a back-to-back lobe in the angular distributions for all values of θ_1, as seen in the leftmost columns of Figs. 7 and 8. An interesting difference between Figs. 7 and 8 is that the $L = 0$ and $L = 2$ components seem to add constructively to the total TDCS in the singlet case, whereas both constructive (for $\theta_1 = 0^\circ$ and $\theta_1 = 30^\circ$) and destructive (for $\theta_1 = 90^\circ$) interferences between the two components are observed in the triplet case.

IV. CONCLUSION AND SUMMARY

Solving the time-dependent Schrödinger equation from first principles, we have studied the process of two-photon double ionization of the helium $1s2s$ singlet and triplet states, taking the full electron-electron interaction into account. The TPDI process has been modeled under two quite different environments, namely, the direct and the RE-TPDI regimes, involving intermediate doubly excited (autoionizing) states in the latter case. Total and differential cross sections are provided in both the singlet and triplet symmetries for various laser photon energies. Regarding the direct process, the total cross section is found to be significantly smaller than the corresponding one related to TPDI of the helium ground state. Furthermore, the TPDI cross section of the $1s2s$ singlet state is almost an order of magnitude bigger than its triplet counterpart. This is attributed to the relative importance of the electron-electron correlation in the different systems, and it is in accordance with the general rule of thumb that the higher the initial-state correlation present in a system is, the higher the cross section expected is. When the $2s2p$ doubly excited state is energetically accessible in the laser field, a cubic relationship between the total probability of double ionization and the pulse duration is demonstrated in the few-femtosecond pulse regime. As such, the $2s2p$ states behave as true bound states on the time

scale of the laser pulses studied here. Differential cross sections have also been presented, and resemblances to similar studies of TPDI in other systems are noted. Whereas the energy-resolved cross section suggests that asymmetric energy sharing is the most dominant outcome for both the singlet and triplet states, the degree of asymmetry is profoundly different when comparing the two. Triple-differential cross sections are shown for both the singlet and triplet target states when the driving field stimulates either direct or resonance-enhanced TPDI. The TDCS reveals an increasing tendency for back-to-back emission with asymmetric energy sharing when the $2s2p$ state is accessible in the field. This is consistent with a comparison of the partial-wave decompositions obtained in the direct and resonance-enhanced TPDI regimes and the fact that the $^{1,3}S^e$ channel has a back-to-back emission pattern. The ionization channels $^{1,3}S^e$ and $^{1,3}D^e$ compete in the resonant case, whereas only $^{1,3}D^e$ is dominant in the direct process. Hence, in the resonant case, this may point to two different ionization routes, i.e., both electrons absorbing one photon each versus the scenario where one electron absorbs two photons.

ACKNOWLEDGMENTS

This work was supported by the Bergen Research Foundation, the Norwegian Metacenter for Computational Science (Notur), the European COST Action CM1204 (XLIC), and the AURORA program [Norges Forskningsråd (NFR) for Norway and ministères des Affaires étrangères (MAE) et de l'Enseignement supérieur et de la Recherche (MESR) for France]. All calculations were performed on the Cray XE6 (Hexagon) supercomputer installation at Parallab, University of Bergen (Norway).

[1] F. W. Byron and C. J. Joachain, Phys. Rev. **164**, 1 (1967).
[2] M. Hentschel, R. Kienberger, C. Spielmann, G. A. Reider, N. Milosevic, T. Brabec, P. Corkum, U. Heinzmann, M. Drescher, and F. Krausz, Nature (London) **414**, 509 (2001).
[3] P. M. Paul, E. S. Toma, P. Breger, G. Mullot, F. Augé, P. Balcou, H. G. Muller, and P. Agostini, Science **292**, 1689 (2001).
[4] T. Shintake, H. Tanaka, T. Hara, T. Tanaka, K. Togawa, M. Yabashi, Y. Otake, Y. Asano, T. Bizen, T. Fukui *et al.*, Nat. Photonics **2**, 555 (2008).
[5] W. Ackermann, G. Asova, V. Ayvazyan, A. Azima, N. Baboi, J. Bähr, V. Balandin, B. Beutner, A. Brandt, A. Bolzmann *et al.*, Nat. Photonics **1**, 336 (2007).
[6] J. A. R. Samson, W. C. Stolte, Z.-X. He, J. N. Cutler, Y. Lu, and R. J. Bartlett, Phys. Rev. A **57**, 1906 (1998).
[7] L. Malegat, P. Selles, and A. K. Kazansky, Phys. Rev. Lett. **85**, 4450 (2000).
[8] J. Colgan and M. S. Pindzola, Phys. Rev. Lett. **88**, 173002 (2002).
[9] S. Laulan and H. Bachau, Phys. Rev. A **68**, 013409 (2003).
[10] B. Piraux, J. Bauer, S. Laulan, and H. Bachau, Eur. Phys. J. D **26**, 7 (2003).
[11] S. X. Hu, J. Colgan, and L. A. Collins, J. Phys. B **38**, L35 (2005).
[12] E. Foumouo, G. L. Kamta, G. Edah, and B. Piraux, Phys. Rev. A **74**, 063409 (2006).
[13] R. Shakeshaft, Phys. Rev. A **76**, 063405 (2007).
[14] D. A. Horner, F. Morales, T. N. Rescigno, F. Martín, and C. W. McCurdy, Phys. Rev. A **76**, 030701(R) (2007).
[15] L. A. A. Nikolopoulos and P. Lambropoulos, J. Phys. B **40**, 1347 (2007).
[16] J. Feist, S. Nagele, R. Pazourek, E. Persson, B. I. Schneider, L. A. Collins, and J. Burgdörfer, Phys. Rev. A **77**, 043420 (2008).
[17] X. Guan, K. Bartschat, and B. I. Schneider, Phys. Rev. A **77**, 043421 (2008).
[18] X. Guan, O. Zatsarinny, C. J. Noble, K. Bartschat, and B. I. Schneider, J. Phys. B **42**, 134015 (2009).
[19] R. Nepstad, T. Birkeland, and M. Førre, Phys. Rev. A **81**, 063402 (2010).
[20] M. Førre, S. Selstø, and R. Nepstad, Phys. Rev. Lett. **105**, 163001 (2010).
[21] A. Palacios, T. N. Rescigno, and C. W. McCurdy, Phys. Rev. A **79**, 033402 (2009).
[22] A. Palacios, D. A. Horner, T. N. Rescigno, and C. W. McCurdy, J. Phys. B **43**, 194003 (2010).
[23] H. Bachau, Phys. Rev. A **83**, 033403 (2011).
[24] A. S. Simonsen, S. Askeland, and M. Førre, Cent. Eur. J. Phys. **11**, 10991106 (2013).
[25] W.-C. Jiang, L.-Y. Peng, W.-H. Xiong, and Q. Gong, Phys. Rev. A **88**, 023410 (2013).
[26] H. Hasegawa, E. J. Takahashi, Y. Nabekawa, K. L. Ishikawa, and K. Midorikawa, Phys. Rev. A **71**, 023407 (2005).
[27] Y. Nabekawa, H. Hasegawa, E. J. Takahashi, and K. Midorikawa, Phys. Rev. Lett. **94**, 043001 (2005).
[28] P. Antoine, E. Foumouo, B. Piraux, T. Shimizu, H. Hasegawa, Y. Nabekawa, and K. Midorikawa, Phys. Rev. A **78**, 023415 (2008).
[29] A. A. Sorokin, M. Wellhöfer, S. V. Bobashev, K. Tiedtke, and M. Richter, Phys. Rev. A **75**, 051402(R) (2007).
[30] A. Rudenko, L. Foucar, M. Kurka, T. Ergler, K. U. Kühnel, Y. H. Jiang, A. Voitkiv, B. Najjari, A. Kheifets, S. Lüdemann *et al.*, Phys. Rev. Lett. **101**, 073003 (2008).
[31] M. Kurka, J. Feist, D. A. Horner, A. Rudenko, Y. H. Jiang, K. U. Kühnel, L. Foucar, T. N. Rescigno, C. W. McCurdy, R. Pazourek *et al.*, New J. Phys. **12**, 073035 (2010).
[32] J. Colgan, M. S. Pindzola, and F. Robicheaux, J. Phys. B **41**, 121002 (2008).
[33] F. Morales, F. Martín, D. A. Horner, T. N. Rescigno, and C. W. McCurdy, J. Phys. B **42**, 134013 (2009).
[34] X. Guan, K. Bartschat, and B. I. Schneider, Phys. Rev. A **84**, 033403 (2011).
[35] X. Guan, K. Bartschat, and B. I. Schneider, Phys. Rev. A **82**, 041404(R) (2010).
[36] A. S. Simonsen, S. A. Sørngård, R. Nepstad, and M. Førre, Phys. Rev. A **85**, 063404 (2012).
[37] I. A. Ivanov and A. S. Kheifets, Phys. Rev. A **87**, 023414 (2013).
[38] X. Guan, K. Bartschat, B. I. Schneider, and L. Koesterke, Phys. Rev. A **88**, 043402 (2013).
[39] Sh. A. Abdel-Naby, M. F. Ciappina, M. S. Pindzola, and J. Colgan, Phys. Rev. A **87**, 063425 (2013).

[40] Z. J. Teng and R. Shakeshaft, Phys. Rev. A **49**, 3597 (1994).
[41] H. W. van der Hart, K. W. Meyer, and C. H. Greene, Phys. Rev. A **57**, 3641 (1998).
[42] J. Colgan and M. S. Pindzola, Phys. Rev. A **67**, 012711 (2003).
[43] K. Stefańska, F. Reynal, and H. Bachau, Phys. Rev. A **85**, 053405 (2012).
[44] A. S. Simonsen, H. Bachau, and M. Førre, Phys. Rev. A **89**, 021405(R) (2014).
[45] S. Askeland, S. A. Sørngård, I. Pilskog, R. Nepstad, and M. Førre, Phys. Rev. A **84**, 033423 (2011).
[46] S. A. Sørngård, S. Askeland, R. Nepstad, and M. Førre, Phys. Rev. A **83**, 033414 (2011).
[47] R. Nepstad and M. Førre, Phys. Rev. A **84**, 021402(R) (2011).
[48] J. Colgan, M. S. Pindzola, and F. Robicheaux, J. Phys. B **34**, L457 (2001).
[49] L. B. Madsen and P. Lambropoulos, Phys. Rev. A **59**, 4574 (1999).
[50] E. Lindroth, Phys. Rev. A **49**, 4473 (1994).
[51] S. Laulan, H. Bachau, B. Piraux, J. Bauer, and G. L. Kamta, J. Mod. Opt. **50**, 353 (2003).
[52] E. Foumouo, A. Hamido, P. Antoine, B. Piraux, H. Bachau, and R. Shakeshaft, J. Phys. B **43**, 091001 (2010).
[53] E. Foumouo, P. Antoine, B. Piraux, L. Malegat, H. Bachau, and R. Shakeshaft, J. Phys. B **41**, 051001 (2008).
[54] F. Maulbetsch and J. S. Briggs, J. Phys. B **28**, 551 (1995).
[55] G. S. J. Armstrong and J. Colgan, Phys. Rev. A **86**, 023407 (2012).